Hot cracking in tungsten inert gas welding of magnesium alloy AZ91D

W. Zhou*, T. Z. Long and C. K. Mark

Plates of 3–5 mm in thickness were extracted from an AZ91D ingot and then butt joints of the plates were produced using tungsten inert gas (TIG) welding method. The TIG arc was also used to deposit welding beads on some of the thin plates. No cracking was found in the butt joints. However, hot cracking was always observed to propagate from the heat affected zone (HAZ) under the welding bead into the weld metal right after a welding bead was deposited on the thin plate. Metallographic and fractographic evidence was obtained to show that the hot cracking is 'liquation cracking' in the partially melted HAZ under the high thermal stresses. In the butt joints, the weld metal has the finest grains, highest strength and best ductility, and the HAZ was found to be the 'weakest link'.

Keywords: Magnesium alloy, AZ91D, TIG welding, Hot cracking, Liquation, Fracture

Introduction

Magnesium alloys have high strength/weight ratio compared with other metals and excellent recyclability compared with plastics. Because of the increasingly stringent environment regulation, limited natural resources and the demand for energy saving, the use of 'ultralight' magnesium alloys is steadily gaining importance, especially in the automobile industry.[1,2] Magnesium alloy AZ91D is widely used because of its relatively higher corrosion resistance and mechanical strength. Considerable researches have been carried out to study optimisation of die casting parameters,[3,4] corrosion resistance[5–8] and mechanical properties[9] of AZ91D magnesium alloys. Effort has also been made, especially in recent years, to solve problems in joining various magnesium alloys.[10–20] However, there has been limited information in published literature concerning the tungsten inert gas (TIG) welding of AZ91D.[13–16]

Previous researches have identified porosity as a major problem in welding of AZ91D die castings.[10,11] Hot cracking is also known as one of the problems in joining magnesium alloys,[12] but the problem is rarely reported in literature on welding of magnesium alloy AZ91D. This is because most of the researchers used high energy density welding methods such as laser beam welding and electron beam welding.[10,11,17,18,21] Hot cracking does not pose as serious a problem when high energy density welding methods are used because the low net heat input causes relatively low distortion and therefore less stresses.

It is noted that high energy density welding facilities are not easily available, so TIG welding method is often used in engineering practice. Much higher energy input has to be used in TIG welding, so the welding stresses produced are expected to be higher and this makes cracking during welding more likely. Whether or not hot cracking occurs during welding depends on the competition between the material's resistance to fracture and the mechanical driving force for cracking. In the present investigation, hot cracking was observed when an AZ91D magnesium alloy was bead-on-plate welded using TIG method. The present paper presents the experimental results and analyses the causes for the problem.

Experimental

The material used in the study was an as cast AZ91D magnesium ingot, whose chemical composition is shown in Table 1. The ingot was sliced into plates of about 3–5 mm in thickness and $\sim 100 \times 50$ mm in size using a band saw. A Miller Shopmaster TIG welding machine was used to weld the magnesium plates in the form of butt joints. In some cases, welding beads were deposited on the plates for metallurgical study. Before welding, sand paper was used to remove the oil and dirt on the surface of the plates. This was found to help to prevent the formation of porosity in the welds.

The welding was conducted using alternating current at a voltage of 20–22 V and current in a range from 60 to 120 A. The welding torch was attached onto an autorunning machine in order to make it travel at a constant speed of ~ 5 mm s^{-1}. The welding was autogenous and no filler rod was ever used.

Metallographic samples were extracted from the base plate and welded joints, etched in ethylene glycol solution (20 mL acetic acid, 60 mL ethylene glycol, 1 mL HNO_3 and 20 mL water) for 30–50 s, and observed using the scanning electron microscopes (SEM). The distributions of alloy elements in all samples

School of Mechanical and Aerospace Engineering, Nanyang Technological University, 50 Nanyang Avenue, Singapore 639798

*Corresponding author, email WZhou@Cantab.Net

Published by Maney on behalf of the Institute
Received 7 August 2006; accepted 20 March 2007
DOI 10.1179/174328407X213026

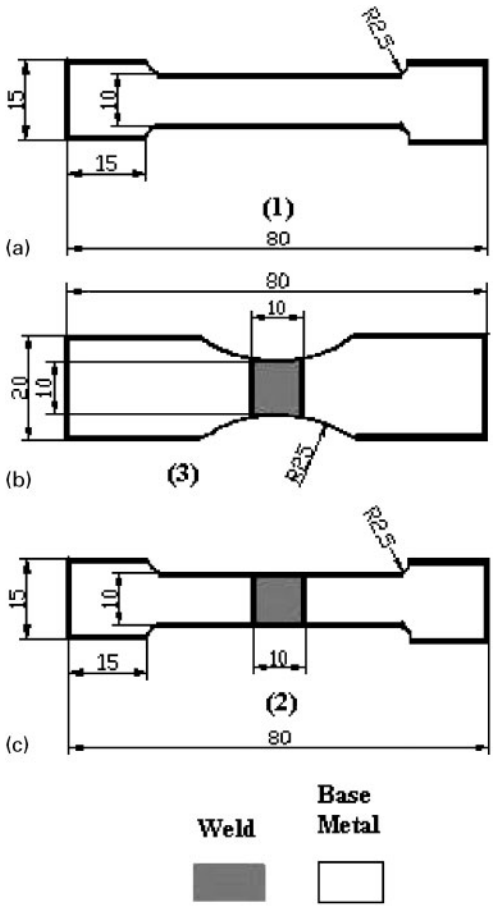

a type 1, used to study properties of ingot; *b* type 2, used to find weakest link in welded joints; *c* type 3, designed to test tensile properties of weld metal

1 Three types of tensile test specimens used

were measured with energy dispersive X-ray spectroscopy (EDX).

Tensile test was performed using an Instron machine of 50 kN capacity at a ramp rate of 1 mm min^{-1} to study mechanical properties of the welded joints. Three types of tensile specimens, as shown in Fig. 1, were made using a computer numerical control (CNC) machine. Specimen type 1 was machined entirely from the AZ91D ingot for studying tensile properties of the base metal. Specimen type 2 contained the welded joint in the parallel zone and was used to find out the weakest link in the joint. Specimen type 3 was designed in a way to place the weld metal in the reduced zone in order to obtain tensile properties of the weld metal. Thickness of all the tensile specimens is 3 mm. Fracture surfaces of the tested specimens and the cracking surface of welded plates were observed using SEM.

Results and discussion

Microstructures

Figure 2 shows the binary Mg–Al phase diagram. According to the diagram, the equilibrium microstrcuture of

Table 1 Chemical composition of AZ91D ingot, wt-%

Al	Mn	Ni	Cu	Zn	Ca	Si	K	Fe	Mg
9·0	0·17	0·001	0·001	0·64	<0·01	<0·01	<0·01	<0·001	Bal.

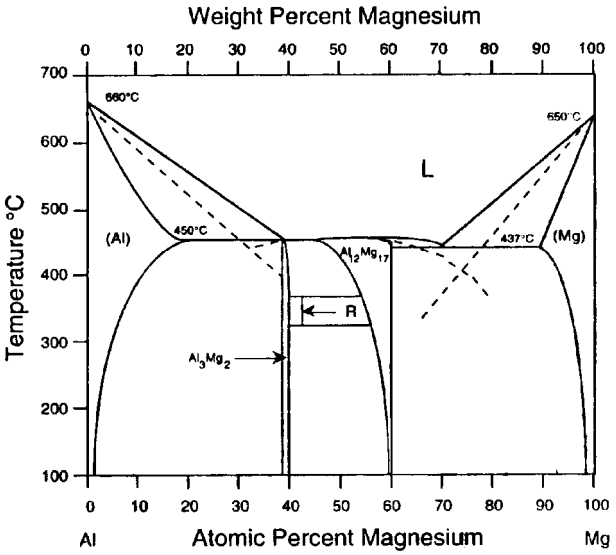

2 Mg–Al phase diagram[22]

AZ91D alloy consists of α-Mg and β ($Al_{12}Mg_{17}$) intermetallic precipates. However, the microstructure of AZ91D ingot used in the present study is different due to non-equilibrium phase transformation. When the ingot solidified in the metal mould, the rapid cooling rate shifted the liquidus, solidus and eutectic point in the equilibrium diagram to lower temperatures. As a result, a divorced eutectic phase appeared in the matrix. The microstructure of AZ91D ingot was observed to contain large primary α dendrites and eutectic phase precipitated between the dendritic arms, as shown in Fig. 3*a*. The divorced eutectic phase consists of secondary α (α') and β ($Mg_{17}Al_{12}$).

The distribution of Al and Mg elements in the ingot was measured using EDX. The result indicates that the β phase and its neighbouring area consist of higher percentage of aluminium, as shown in Fig. 3*b*. The aluminium concentration varies from 35 wt-% in the β phase area to 5 wt-% in the centre of the primary α phase.

Cross-section of a bead-on-plate welded joint is shown in Fig. 4. Both weld metal and heat affected zone (HAZ) are shown clearly in the figure. The microstructures in the two zones are also shown at higher magnifications in Fig. 5.

Compared with the coarse grains (~100 μm in diameter) in the base metal (Figs. 3*a* and 5*a*), finest microstructure formed in the weld (Fig. 5*b*–*c*). The fine grains resulted from the rapid cooling rate during welding and the grain size varied with the heat input. When setting the heat input at a constant value (I=100 A, V=22 V), the grain size varied with the variation of welding speed. Grains of 5–10 μm in size formed in the weld at a welding speed of 10 mm s^{-1} (Fig. 5*b*), while the grain size increased to about 15–20 μm when welding speed was reduced to 2 mm s^{-1} (Fig. 5*c*).

It is accepted that in the HAZ, the grains next to the fusion boundary were found to grow larger (Figs. 4 and 5*d*) due to the intensive heat and thus high temperature they experienced during welding. However, in the part of HAZ further away from this zone, the grains were more or less the same in size as in the base metal (Fig. 4).

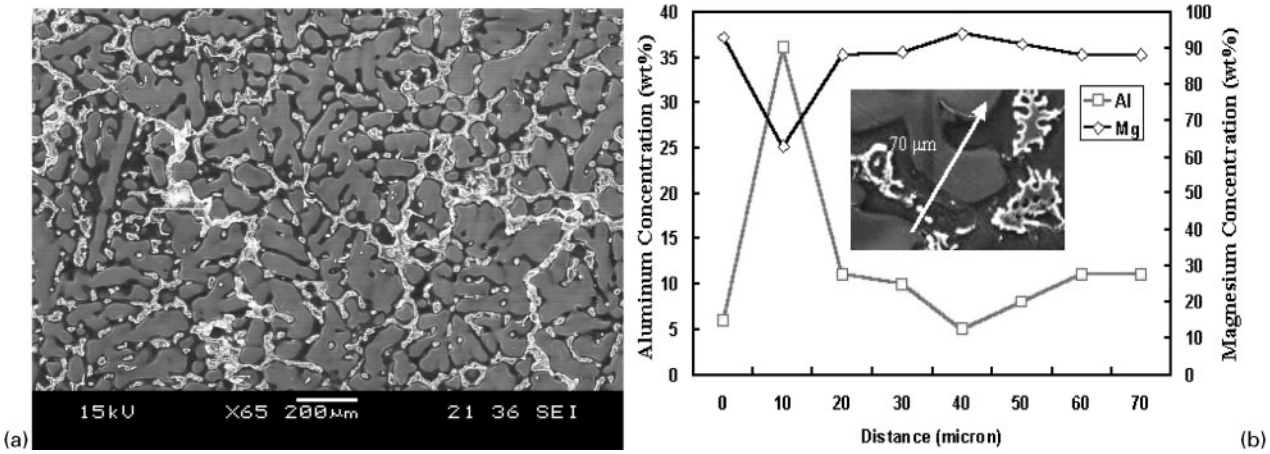

3 ***a*** **microstructure of AZ91D ingot and** ***b*** **Al and Mg element distribution along line shown in SEM image**

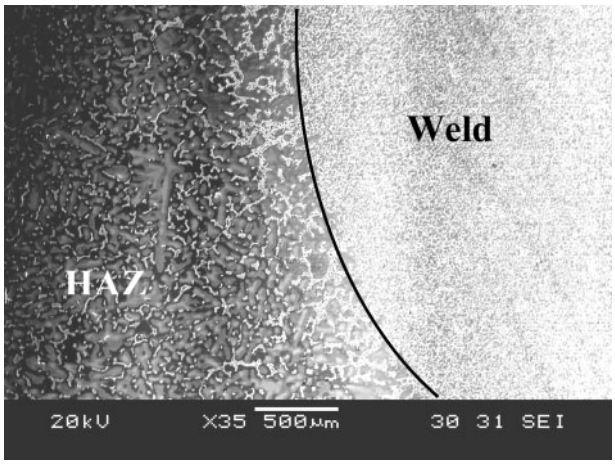

4 Image (SEM) of AZ91D TIG joint showing weld metal and HAZ: microstructure of base metal can be seen in Fig. 3

Chemical composition of the weld metal was found to differ from that of the base metal. EDX analysis shows that the average Al content in the weld is slightly higher (9·2 wt-%) than that of the base metal (9·0 wt-%). The increasing Al content in the fusion zone is believed to result from the loss of magnesium during welding operation because magnesium has a high vapour pressure at high temperatures and it will evaporate easily during welding.

During welding, the microstructures in the HAZ are exposed to high temperatures ranging from the eutectic temperature to liquidus temperature. Hence, in this region, part of primary α phase and all eutectic phases, including eutectic α phase and eutectic β phase, melted during the welding process. That is to say, the HAZ melts partially during welding. When the partially melted HAZ was cooled after the TIG arc moved away, the cooling rate was faster than the cooling rate

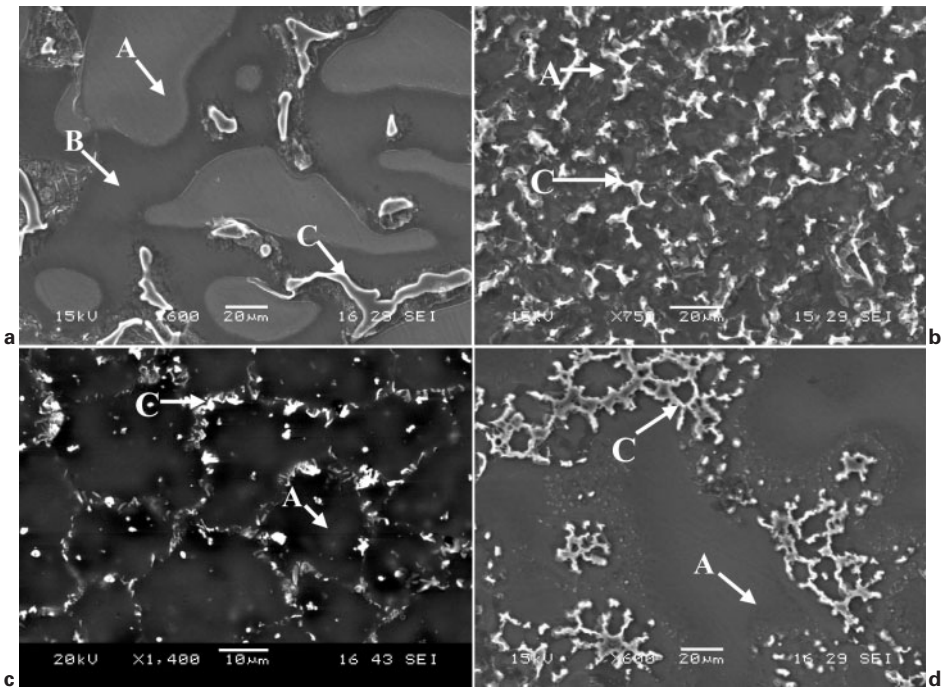

a base metal; ***b*** weld metal produced at welding speed of 10 mm s^{-1} showing fine grains; ***c*** weld metal produced at lower welding speed of 2 mm s^{-1} showing fine but larger grains; ***d*** coarse grained HAZ close to fusion boundary

5 Microstructures in different zones of weld joint: symbols A, B and C represent primary α, eutectic α and eutectic β respectively

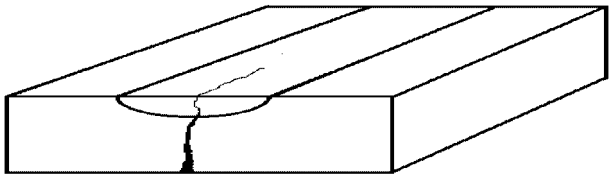

6 Illustration of hot cracking in bead-on-plate welded AZ91D plate

experienced by the base metal during the ingot cooling; therefore, more β phase precipitated along the grain boundaries, as shown in Fig. 5*d*. Stern and Munitz[13] and Munitz *et al.*[14] studied TIG welding of AZ91D alloy and reported a partially melted zone of >2 mm in width. In the present research, the width of HAZ was found to be >3 mm.

Hot cracking in bead-on-plate welded joint

No cracking was observed in the welded joint after butt welding of two AZ91D plates. However, right after deposition of a welding bead on plate, cracking invariably occurred in the joint. The cracking formed at high temperatures, so it is a type of hot cracking. The appearance of the cracking is highly repeatable in all specimens, as illustrated in Fig. 6. The crack profile indicates that cracking initiated under the welding bead and then propagated into the weld metal.

Classical theories about the mechanisms of hot cracking were developed by Borland[23] and Prokhorov.[24] Hot cracking is generally classified into two categories: solidification cracking which forms in the weld, and liquation cracking which occurs in the HAZ. According to Provkhorov's theory,[24] 'solidification cracking' occurs in 'brittle temperature range (BTR)' during the solidification of the weld metal. In BTR, the liquid film existing between the grains greatly decreased the strength of the weld. When the thermal strain or strain rate developed during welding surpasses the material's endurance, 'solidification cracking' forms in the weld.

Liquation cracking formed in the HAZ of the joint relates to the liquation of second phase or low melting point precipitates in the matrix. Liquation cracking may occur in HAZ subjected to tensile stresses if the low melting microstructures in the zone melt partially at high temperatures during welding.[25] Since the hot cracks were observed to initiate under the welding bead (e.g. outside the weld) and then propagate into the weld metal, the cracking is very likely to be of 'liquation cracking' type.

Metallurgical factor and mechanical factor are always the two main factors causing crack formation. Therefore, metallographic observation and stress analysis were carried out to study the hot cracking phenomenon further.

Metallurgical factor

Metallographic samples were sectioned from the cracked joints and observed under the SEM after grinding, polishing and etching. Special attention was paid to HAZ under the weld bead since hot cracking was observed to initiate from there. The hot crack was found to propagate along the eutectic phase in HAZ, as shown in Fig. 7.

It can be seen clearly from Fig. 7 that the microstructures along the hot cracking path are very different

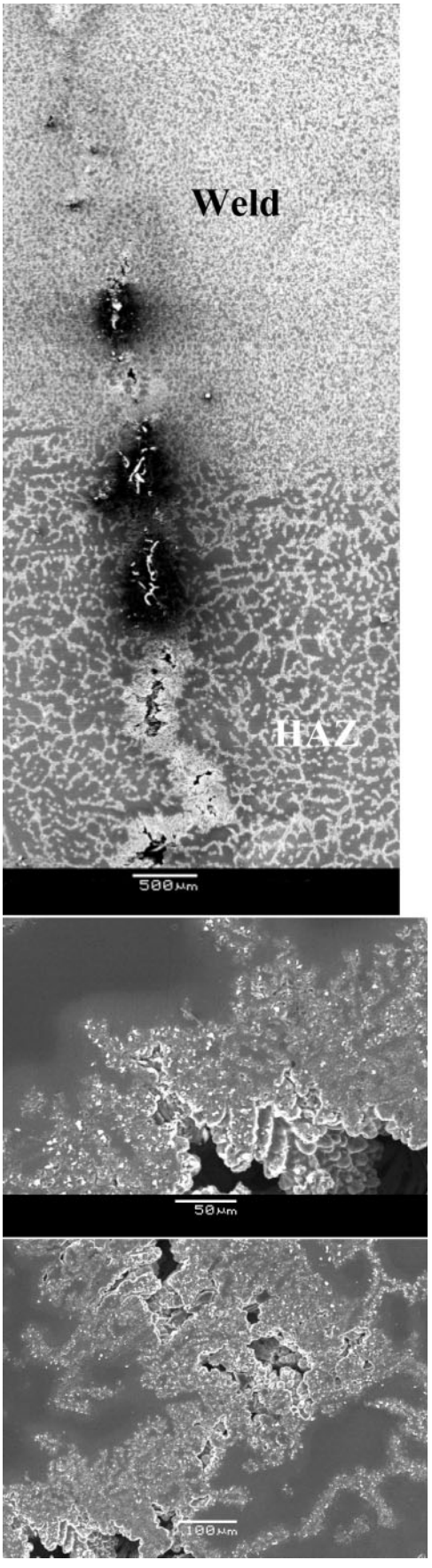

7 *a* hot cracking in bead-on-plate welding, note that crack was arrested in weld and *b–c* close-up of hot crack path showing eutectic phase in form of dendritic structure

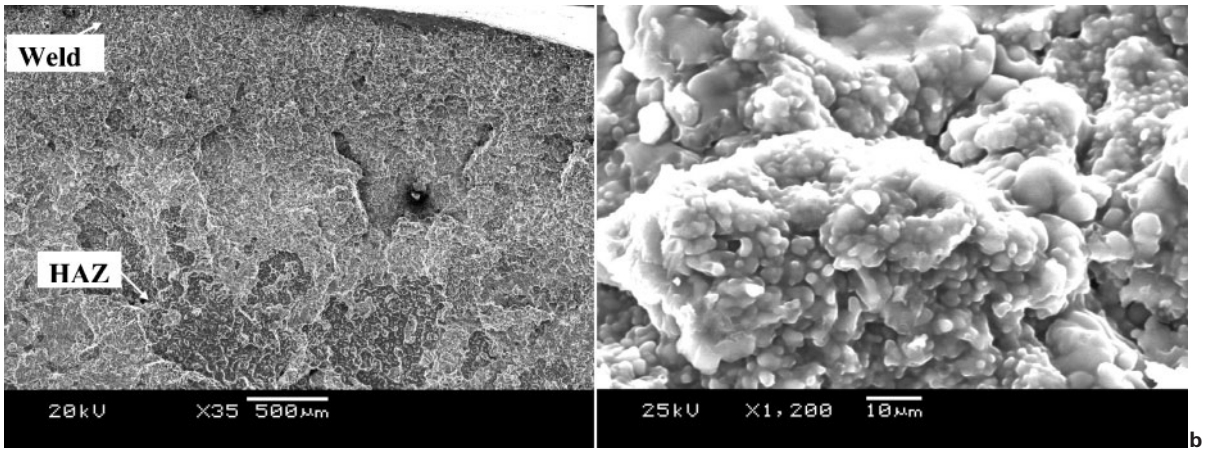

8 ***a*** **hot cracking surface in HAZ (lower part) and weld fracture surface and** ***b*** **close-up of hot cracking surface showing very fine grains: note that grains are finer than those in normal HAZ by order of magnitude (*see* Figs. 7*a* and 9*a*)**

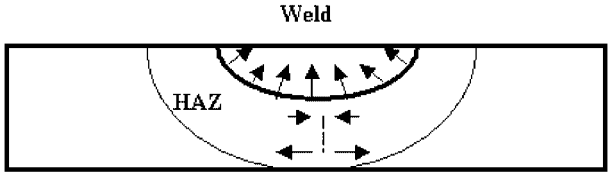

9 Stress distribution in bead-on-plate joint during solidification and contraction of weld metal: note that large part of HAZ is in tension

from those in other parts of HAZ (also refer to Fig. 4). In the HAZ at a distance away from the weld bead, high volume of eutectic phase precipitates in the form of dendrites were found along the hot crack path, as shown in Fig. 7*b–c*. The formation of dendrites indicates that the hot cracking was due to partial melting of microstructures in the HAZ.

Typical fractographs of hot cracking are shown in Fig. 8*a–b*. Compared with the tensile fracture surface of the HAZ of butt welded joints (shown later in Fig. 10*a*), the hot cracking surface is seen to have considerably finer size grains (roughly by an order of magnitude). The much finer grains observed on the hot cracking surface can only be attributed to resolidification of partially melted microstructures in HAZ. This again indicates that the formation of hot cracks is due to partial melting in HAZ.

Mechanical factor

Magnesium alloys have a high thermal conductivity (156 W m^{-1} K^{-1} at 27°C) and low specific heat capacity (1025 J kg^{-1} K^{-1} at 20°C).[26] Therefore, HAZs in welded joints of magnesium alloys are usually very wide. In the present research, the width of HAZ was found to be >3 mm. Considering that the welding bead depth is ~2 mm, for the 3–5 mm thick plates used, the whole section under the weld bead is in fact partially melted HAZ.

Butt joints also contain wide HAZs, but no cracking was observed in those joints. Therefore, metallurgical factor alone cannot cause the cracking. Mechanical factor has to be considered. During butt welding, the plates could expand and contract easily, and this resulted in low thermal stresses. In contrast, when a weld bead was deposited on a plate, large tensile stresses built up in a large part of HAZ under the weld bead when the weld metal solidified and contracted, as illustrated in Fig. 9. It is worthwhile to note that magnesium alloys have high thermal expansion coefficient ($16{\cdot}1 \times 10^{-6}$°C between 20 and 400°C),[26] so the tensile stresses in the HAZ are expected to be high.

Mechanical properties of butt welded joints

Table 2 lists the tensile test results for the three types of specimens. It shows clearly that the weld metal has not only higher ultimate tensile strength (UTS) but also larger elongation compared with the base metal. This result is not surprising since the weld metal was observed to contain much finer grains (Fig. 5).

Type 2 specimens were designed to find the 'weakest link' in the butt joints. For all the nine type 2 specimens tested, fracture was observed to occur in HAZs. This demonstrates that the HAZs are the weakest link in the welded joints. However, it should be noted that both strength and ductility of the HAZs are very close to those of the base metal. Fractographic observation under the SEM revealed largely intergranular fracture for both base metal and HAZ, as shown in Fig. 10*a* and *b*. In contrast, the fine grained weld metal was observed to break transgranularly with dimples on the fracture surfaces, as shown in Fig. 10*c*.

Summary and conclusions

AZ91D plates can be successfully butt welded using TIG welding method. No cracking was found in the butt joints. However, hot cracking was always observed to

Table 2 Tensile properties of three types of tensile specimens

Specimen type	UTS, MPa	Elongation, %	Observations
Type 1	160±15	5·3±0·3	Six base metal specimens were tested
Type 2	156±20	5·1±0·3	Fracture occurred in HAZ for all the 9 specimens tested.
Type 3	240±20	6·8±0·4	Fracture occurred within weld metal for all the 7 specimens tested.

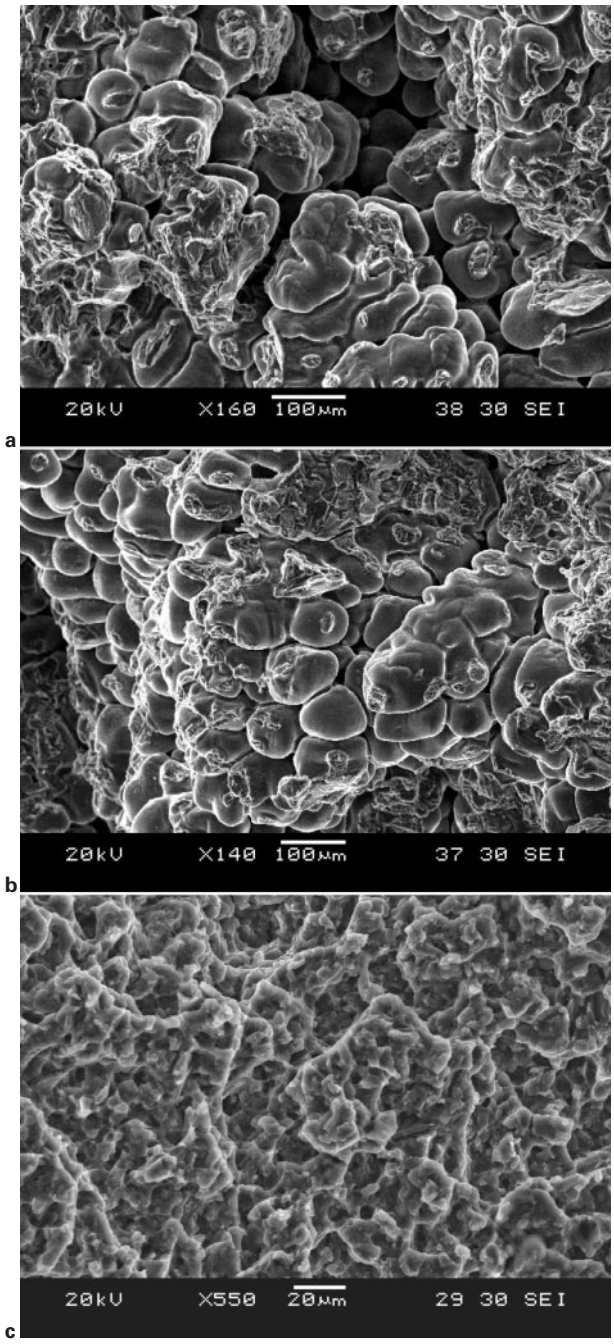

10 Fractographs (SEM) showing typical fracture surfaces for *a* HAZ, *b* base metal and *c* weld metal

propagate from the HAZ under the welding bead into the weld metal right after a welding bead was deposited on the thin plate. The cracking is believed to be 'liquation cracking' in the partially melted HAZ under the high thermal stresses.

Among the three zones in the AZ91D welded joints, the weld metal has the finest grains and thus highest UTS and elongation to fracture. Weld metal broke transgranularly. In contrast, fracture of base metal and HAZ is intergranular. The HAZ was found to be the 'weakest link' in the welded joint but its strength and ductility are very close to those of the base metal.

It should be noted that the work was carried out on plates cut from cast ingots and not on die cast plates, thus avoiding the porosity problem. Further work needs to be carried out to assess the suitability of the TIG welding technique for AZ91D die castings.

References

1. T. J. Ruden and D. L. Albright: *Adv. Mater. Process.*, 1994, **145**, (6), 28–32.
2. R. VanFleteren: *Adv. Mater. Process.*, 1996, **149**, (5), 33–34.
3. Y. B. Li and W. Zhou: *Mater. Technol.*, 2003, **18**, (1), 36–41.
4. Y. J. Huang, B. H. Hu, I. Pinwill, W. Zhou and D. M. R. Taplin: *Mater. Manufact. Process.*, 2000, **15**, (1), 97–105.
5. N. N. Aung and W. Zhou: *J. Appl. Electrochem.*, 2002, **32**, (12), 1397–1401.
6. R. Ambat, N. N. Aung and W. Zhou: *Corros. Sci.*, 2000, **42**, 1433–1455.
7. R. Ambat, N. N. Aung and W. Zhou: *J. Appl. Electrochem.*, 2000, **30**, 865–874.
8. G. H. Wu, Y. Fan, H. T. Gao, C. Q. Zhai and Y. P. Zhu: *Mater. Sci. Eng. A*, 2005, **A408**, 255–263.
9. A. Bag and W. Zhou: *J. Mater. Sci. Lett.*, 2001, **20**, 457–459.
10. A. Weisheit, R. Galun and B. L. Mordike: *Weld. J.*, 1998, **77**, (4), 149s–154s.
11. U. Dilthey, A. Brandenburg, G. Trager, H. Haferkamp and M. Niemeyer: *Materialwiss. Werkst.*, 1999, **30**, (11), 682–692.
12. American Welding Society: 'Welding handbook', 7th edn, Vol. 4, 396; 1989, Miami, FL, AWS.
13. A. Stern and A. Munitz: *J. Mater. Sci. Lett.*, 1999, **18**, (11), 853–855.
14. A. Munitz, C. Cotler, A. Stern, and G. Kohn: *Mater. Sci. Eng. A*, 2001, **A302**, (1), 68–73.
15. L. M. Liu, Z. D. Zhang, Y. Shen and L. Wang: *Acta Metall. Sin.*, 2006, **42**, 399–404.
16. L. M. Liu, Z. D. Zhang, G. Song and Y. Shen: *Mater. Trans.*, 2006, **47**, 446–449.
17. X. Cao, M. Jahazi, J. P. Immarigeon and W. Wallace: *J. Mater. Process. Technol.*, 2006, **171**, 188–204.
18. C. T. Chi, C. G. Chao, C. A. Huang and C. H. Lee: *Mater. Sci. Forum*, 2006, **505–507**, 193–198.
19. T. P. Zhu, Z. W. Chen and W. Gao: *Mater. Sci. Eng. A*, 2006, **A416**, 246–252.
20. J. C. Feng, Y. R. Wang and Z. D. Zhang: *Sci. Technol. Weld. Join.*, 2006, **11**, 154–162.
21. A. Munitz, C. Cotler, H. Shaham and G. Kohn: *Weld. J.*, 2000, **79**, (7), 202s–208s.
22. A. A. Nayeb-Hashemi and J. B. Clark: 'Phase diagrams of binary magnesium alloys', 18; 1988, Metals Park, OH, ASM International.
23. J. C. Borland: *Brit. Weld. J.*, 1961, **8**, 526–540.
24. N. N. Prokhorov: *Weld. Product.*, 1962, **9**, (4), 1–8.
25. B. Radhakrishnan and R. G. Thompson: *Metall. Trans. A*, 1992, **A23**, (6), 1783–1799.
26. M. M. Avedesian: 'Magnesium and magnesium alloys', 8–9; 1999, Materials Park, OH, ASM International.